 CMC, vol.18, no.2, pp.183-211, 2010

Numerical Study of PVB Laminated Windshield Cracking Upon Human Head Impact

Jun Xu[1,2], Yibing Li[1], Xi Chen[2,3], Yuan Yan[2,3], Dongyun Ge[4] Mengyi Zhu[1] and Bohan Liu[1]

Abstract: The crack pattern in a PVB laminated windshield upon head impact is of considerable interest because it contains important information on energy mitigation, pedestrian protection, and accident reconstruction. We carry out a systematic numerical study based on the extended finite element method (XFEM), to investigate the effects of various material and system variables, including the impact speed, effective head mass, PVB interlayer material thickness and property, windshield curvature, aspect ratio and size, boundary constraint, impact angle and off-center impact, on the parameters characterizing the resulting crack pattern, i.e. the crack length, crack angle and circumferential crack shape. General relations bridging these variables and parameters are established via extensive simulations, and the effect and mechanism of each governing factor are elucidated. The findings will shed some light on accident investigation, crashworthiness, and vehicle safety design, on the basis of a systematic understanding of the PVB laminated windshield cracking subject to human head impact.

Keywords: PVB laminated windshield; Extended finite element method; Low-speed impact; Crack pattern

1 Introduction

PVB laminated windshield is widely used in modern automobiles [Valera and Demarquette (2008)] including passenger vehicles. Cracks may appear on the windshield if it undergoes external impact; during an accident involving a vehicle and a pedestrian or between two vehicles, the foreign object is usually the pedestrian

[1] State Key Laboratory of Automotive Safety & Energy, Department of Automotive Engineering, Tsinghua University, Beijing , P.R .China
[2] Department of Earth and Environmental Engineering, Columbia University, NY, USA
[3] School of Aerospace, Xi'an Jiaotong University, Xi'an, P.R .China
[4] School of Aerospace, Tsinghua University, Beijing, P.R .China

head or passenger head. The study of PVB laminated windshield cracking features upon human head impact is therefore, useful for pedestrian and passenger protection [Wei and Dharani (2006); Xu and Li (2009)], vehicular crashworthiness design [Jacob, Starbuck, Fellers, Simunovic and Boeman (2006); Van Slycken, Verleysen, Degrieck, Bouquerel and De Cooman (2006)] and accident reconstruction [Xu, Du, Xu, Wang and Lin (2008); Xu, Li, Lu and Zhou (2009)].

The PVB laminated windshield can be typically modeled as a viscoelastic interlayer (PVB) sandwiched by two glass layers. Previous studies on such a composite structure can be categorized into theoretical constitutive relations, numerical simulations (mostly based on the finite element analysis (FEA)), and experiments. Among previous theoretical efforts, Asik et al. [Asik and Tezcan (2005)] established a constitutive model based on the minimum potential energy principle and investigated multiple factors that could affect the strength [Asik and Tezcan (2006)]. A laminated glass model based on the Kirchhoff plate theory was developed by Akrout [Akrout, Hammami, Tahar and Haddar (2008)]. Although these theoretical explorations may provide a basis for numerical simulation and help to explain experimental result, they do not involve any study of crack initiation and propagation.

Experimentally, quasi-static tests on both OEM and modified glazing systems were done by Herndon [Herndon, Allen, Roberts, Phillips and Batzer (2007)], which showed that the glazing system could still carry load after glass cracking. The damage evolution in a laminated glass plate was investigated by Seshadri et al. [Seshadri, Bennison, Jagota and Saigal (2002)], and Muralidhar et al. [Muralidhar, Jagota, Bennison and Saigal (2000)] and Rahulkumar et al. [RahulKumar, Jagota, Bennison and Saigal (2000)] further investigated the debonding at the glass-polymer interface. Unfortunately, experimental study on the fracture characteristics of PVB laminated windshield is still lacking.

Numerical simulations have been widely used to study impact on windshields and provide useful insights for both theoretical and experimental investigations. Using a continuum damage mechanics model, Zhao and Dharani [Zhao, Dharani, Chai and Barbat (2006); Zhao, Dharani, Chai and Barbat (2006); Zhao, Dharani, Liang, Chai and Barbat (2005)] investigated the dynamic response to human head impact and identified the potential damage domain. A similar damage mechanics analysis was carried out by Sun et al. [Sun and Khaleel (2005)] for studying the stone-impact resistance of windshield, and the damage distribution was obtained. Du Bois et al. and Timmel et al. [Du Bois, Kolling and Fassnacht (2003); Sun, Liu, Chen and Templeton (2009); Timmel, Kolling, Osterrieder and Bois (2007)] used a smeared model based on an explicit finite element solver to compute the dynamic stress distribution of the windshield before and after fracture. Ivanov [Ivanov (2006)]

explored the PVB-glass interaction by FEA and found that the shear stress in the PVB layer played a dominate role in mechanical integrity. Note that these previous numerical studies did not involve explicit crack growth and pattern analysis.

Recently, we [Xu, Li, Chen, Yan, Ge, Zhu and Liu (2010)] employed the extended finite element method (XFEM) [Belytschko and Black (1999); Moes, Dolbow and Belytschko (1999)] to study the fracture pattern on a model glass windshield upon head impact, and correlated that with the real-world accident. The advantage of XFEM is that the crack advancement can be simulated without the need to remesh. Due to the more prominent hoop stress field, radial crack first grows along a particular angle and its length and angle depend on the impact condition and boundary constraint. Next, to release the excessive radial stress, circumferential crack would develop both near the contact zone and at the perimeter of previous radial crack. The sequences of crack growth are consistent with experiments [Xu and Li (2009); Xu, Li, Lu and Zhou (2009)]. The effects of impact speed and effective head mass were studied and correlated with the crack direction and length [Xu, Li, Chen, Yan, Ge, Zhu and Liu (2010)]. The robustness of the XFEM simulation was explored regarding the sensitivity to initial material flaw and material fracture criterion, etc. Despite its initial success for validating the applicability of XFEM for head-windshield impact problem, the windshield model in the previous study [Xu, Li, Chen, Yan, Ge, Zhu and Liu (2010)] was perhaps over simplified since it did not contain the important PVB layer (instead only a pure glass was studied), and the windshield was absent of curvature (which can be important for the resulting impact stress field/crack pattern), and other potentially important factors such as the boundary condition of windshield, off-center impact and inclined impact (which are common in real-world accidents), were not discussed.

In order to provide useful implications on accident reconstruction, pedestrian protection, and vehicle crashworthiness analysis, a systematic numerical simulation of the crack propagation and pattern in a PVB laminated windshield may serve as a first effort to fill the gap mentioned above. In this paper, we apply the XFEM approach to simulate fracture characteristics in PVB laminated windshields, whose geometrical and material parameters (e.g. curvature, dimension, PVB properties and thickness, etc.) are varied, as well as boundary constraints, and characteristics of impact (e.g. impact speed, location, angle, and effective head mass etc.), so as to explore their respective effects on cracking behaviors.

2 Model and Methods

2.1 Computational Model

2.1.1 Head model

In real-world pedestrian-vehicle accidents, the interaction between pedestrian and vehicle can be divided into three phases [Xu and Li (2009)]: i) pedestrian-vehicle contact; ii) impact between windshield/engine hood and pedestrian and iii) pedestrian-vehicle separation (either flipping over or sliding down), sketched in Figure 1. Head is the most vulnerable and possible part that gets involved during the impact (phase ii and iii) [Yao, Yang and Otte (2008)]. A featureless headform (Figure 2) with $R_{\text{Head}} = 90mm$ and reference mass of 4.5kg is commonly adopted in windshield testing and evaluation in automotive industry [Zhao, Dharani, Liang, Chai and Barbat (2005)]. While the same model head radius is adopted in this study, we note that the effective head mass depends on the vehicle's impact speed [Wood (1998)], pedestrian-vehicle contact location and front-end shape of vehicle (see Figure 1), thus the effective head mass M_{Head} is varied from 4.5 kg to 90 kg (by fixing the head size and changing its density). The head material is chosen to be consistent with both the featureless headform standard and Ref. [Zhao, Dharani, Chai and Barbat (2006)], i.e. $E_{\text{Head}} = 6.5\text{GPa}$ and $\nu_{\text{Head}} = 0.26$ without any plastic deformation and damage.

2.1.2 Windshield model

For a reference windshield, its in-plane dimension ($a \times b$) is standard 1400mm $\times$ 600mm and without curvature. According to Figure 2, a real windshield may contain a curvature with respect to the z-direction, and the curvature and dimension of the windshield may vary in moderate ranges in different automobiles and thus their effects are explored in detail below.

The reference thickness of the PVB interlayer is typically $t_{\text{PVB}_0} = 0.76\text{mm}$ for passenger cars; in this study, we also vary its thickness (up to 3.04mm) to examine whether changing this parameter may lead to different crashworthiness. The density of PVB material is $\rho_{\text{PVB}} = 1100\text{kg/m}^3$ [Zhao, Dharani, Chai and Barbat (2006)]. The reference stress-strain relationship of the PVB material was obtained from our previous experiment [Xu, Li, Ge, Liu and Zhu (In press)] (see Section 3.1.2 for details). Although PVB is kind of a viscoelastic material, we here ignore the viscoelasticity of PVB acording to the suggestions in Ref. [Xu, Li, Ge, Liu and Zhu (In press)] due to the small viscoelasticity effect. Since the physical properties of PVB may vary with respect to age, temperature, working environment, etc. in this paper we also vary the mechanical properties moderately so as to explore their influences on cracking characteristics.

(a) Pedestrian-vehicle contact phase

(b) Impact between windshield/engine hood and human head

(c) Pedestrian-vehicle separation

Figure 1: Illustration for pedestrian-vehicle accident process

The in-plane dimensions of the two glass layers are the same as that of PVB except the thickness. We adopt the typical thickness of the windshield, $t_{\text{Glass}} = 2\text{mm}$ for each glass sheet. As a matter of fact, the thickness of glass layer seldom changes with respect to different types of vehicles, thus t_{Glass} remains a constant in this study. The typical material parameters of soda-lime glass are density $\rho_{\text{Glass}} = 2500\text{kg}/\text{m}^3$, Young's modulus $E_{\text{Glass}} = 70\text{GPa}$, Poisson's ratio $\nu_{\text{Glass}} = 0.22$, mode I energy release rate $G_{\text{I}} = 10\text{J}/\text{m}^2$, mode II and mode III energy release rates $G_{\text{II}} = G_{\text{III}} = 50\text{J}/\text{m}^2$. These properties are assumed to be rate independent .[Holand and Beall (2002)] and also fixed in the present study (the effects of energy release rate, fracture criterion, and initial flaw were discussed in Ref. [Xu, Li, Chen, Yan,

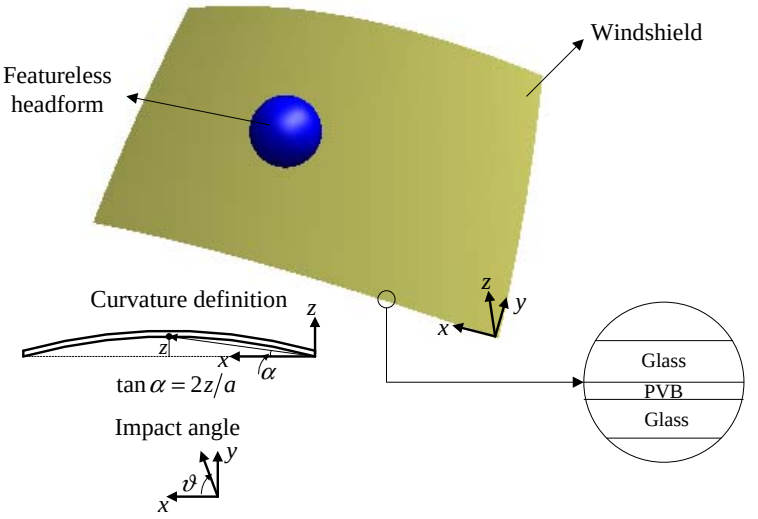

Figure 2: Computational model setup

Ge, Zhu and Liu (2010)]). The size and distribution of initial flaws in the glass have minor effects on the final crack pattern and length (as long as they are sufficiently small comparing with windshield dimension) [Xu, Li, Chen, Yan, Ge, Zhu and Liu (2010)].

2.1.3 Model setup

The contact between the head and top glass sheet is defined as "hard contact" whose impact stress field induces the crack pattern of interest. The Coulomb's friction coefficient between the head and glass is $f = 0.1$, usually a minor factor for resulting contact stress as long as it is nearly frictionless [Ogasawara, Chiba and Chen (2006)]. In most cases we assume the impact occurs normally at the center of the windshield, and we also discuss briefly the effect of off-center impact and inclined impact. If the impact is normal and at the center of the windshield, then only $1/4$ of the system needs to be modeled and analyzed (for example, the result of crack pattern in Figure 4 later in this paper only shows $1/4$ of the windshield); otherwise for general off-center and/or inclined impact, the entire windshield (e.g. that in Figure 2) needs to be taken into account.

Both the head and windshield are meshed with eight-node linear brick elements, and a mesh convergence study is carried out to determine the mesh density, that is 1mm$\times$1mm. For most parts of this study, the boundary condition for the windshield is fixed (clamped), qualitatively consistent with the frame-setup in practice [Yuan

and Li (2005)], and a parametric study on different boundary conditions is also conducted to investigate its influence on cracking properties.

According to the census data from National Traffic Accident Database of Tsinghua University (NTADTU), most of the impact speeds involved in vehicle accidents are between 40 km/h-80 km/h, i.e. 11.1 m/s-22.2m/s, and that is the range of low-speed impact we study in this paper.

2.2 Computational Method

Since our previous study [Xu, Li, Chen, Yan, Ge, Zhu and Liu (2010)] has shown that the dynamic effect is relatively minor for the ranges of parameters we investigate in this paper, we may simplify the low-speed dynamic impact cracking problem into a quasi-static indentation fracture one, and employ the quasi-static indentation stress field to initiate and propagate the radial and circumferential cracks.

For different impact conditions, dynamic FEM simulations (without cracking) are first carried out so as to obtain the equivalent quasi-static indentation conditions. We first limit our attention to normal and center head impacts (and off-center and inclined impacts may be analyzed in similar ways). In addition, we keep other simulation conditions at "regular" reference parameters, i.e. the windshield dimension is standard without curvature, boundary condition is clamped, and PVB properties are kept at their reference values (all reference parameters are listed in Table 1). For different values of the effective head mass M, impact speed v, and thickness of PVB interlayer t_{PVB}, the maximum impact displacement of the head D is computed and presented in a dimensionless form. Finally, D/t ($t = t_{\mathrm{PVB}} + t_{\mathrm{Glass}}$ is the total thickness of windshield) can be fitted as a dimensionless function of v/v_0, M/M_0 and $t_{\mathrm{PVB}}/t_{\mathrm{PVB}_0}$ as

$$\begin{aligned} D/t = &\left[(v/v_0)^{-0.8799} + (M/M_0)^{-3.334} + 0.6679\right]^{-3.338} \\ &+ \left[(M/M_0)^{3.357} + (t_{\mathrm{PVB}}/t_{\mathrm{PVB}_0})^{2.194} + 1.070\right]^{0.07599} \\ &+ \left[(v/v_0)^{0.09454} + (t_{\mathrm{PVB}}/t_{\mathrm{PVB}_0})^{-0.03154} - 1.082\right]^{6.131} - 1.424 \end{aligned} \tag{1}$$

for the range of parameters employed in this study, where $v_0 = \sqrt{G_{\mathrm{I}}/\rho t}$ is the reference velocity, and $M_0 = 9.1\mathrm{kg}$ is the mass of the reference PVB laminated windshield mass using the "regular" parameters mentioned above. The correlation coefficient of fitting is $R = 0.999$ (see Figure 3). In what follows, the normalized displacement D/t can be employed to represent the combined (and coupled) effect of the effective impact mass, center and normal impact speed, and PVB interlayer thickness.

A quasi-static indentation simulation is then carried out (to reach a particular D/t of the "head" indenter) using XFEM, and the resulting stress field is the driving force for the concurrent crack propagation.

For impact-induced windshield fracture, circumferential cracks always grow after the radial cracks that have been developed [Xu and Li (2009); Xu, Li, Lu and Zhou (2009)] (except near the vicinity of impact where extensive damage can be found), because the hoop stress field is more prominent than radial stress. Therefore, we divide the crack simulation based on XFEM into two steps, first the radial crack initiates from the center of windshield (with the assistance of random initial flaws), and next the circumferential crack growth is calculated; more details and the robustness of such an approach are given in [Xu, Li, Chen, Yan, Ge, Zhu and Liu (2010)]. In what follows, a systematic parametric study is carried out by taking into account several major factors that could affect the crack shape, angle, and length, which are the main parameters characterizing the crack pattern.

Table 1: Values of parameters used in a reference windshield model

Parts	Variables	Reference parameters
Head	Mass M_{Head}	4.5kg
	Radius R_{Head}	90mm
	Density ρ_{Head}	1412kg/m^3
	Poisson's ratio ν_{Head}	0.26
	Young's modulus E_{Head}	6.5GPa
Glass	Dimension $a \times b$	1400mm$\times$700mm
	Thickness t_{Glass}	2mm (each layer)
	Density ρ_{Glass}	2500kg/m^3
	Young's modulus E_{Glass}	70GPa
	Poisson's ratio ν_{Glass}	0.22
PVB	Dimension $a \times b$	1400 mm$\times$700 mm
	Thickness t_{PVB}	0.76mm
	Density ρ_{PVB}	1100kg/m^3
Crack settings	Mode I energy release rate G_{I}	10J/m^2
	Mode II energy release rate G_{II}	50J/m^2
	Mode III energy release rate G_{III}	50J/m^2
Global settings	Windshield curvature α	0 degrees
	Boundary conditions	Clamped

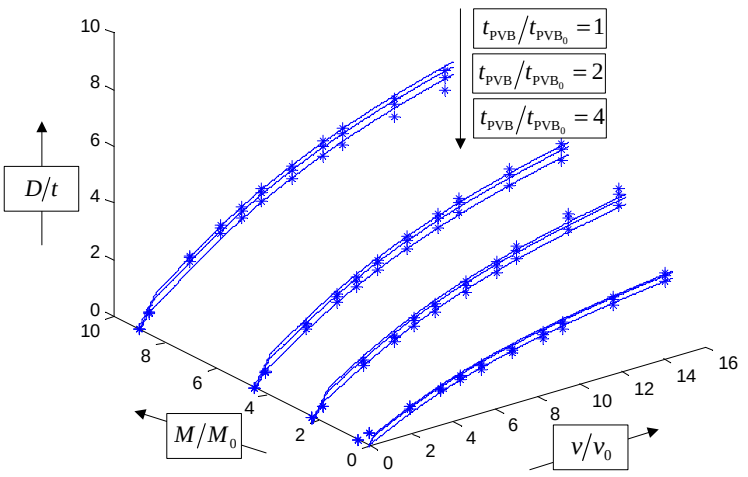

Figure 3: Relationship between the head displacement and initial impact velocity, PVB interlayer thickness and head mass (all parameters are normalized); the lines denoting curve fitting based on Eq. (1).

3 Results and Disccusions

3.1 Effects of PVB interlayer material property

3.1.1 Effect of PVB interlayer thickness

The invention of PVB laminated windshield has contributed significantly to the automotive industry because it has saved many human lives and greatly reduced injuries. In this study, crack patterns and crack lengths are investigated and compared in windshield models with and without the PVB interlayer. In particular, the crack length may be an effective indicator of PVB's energy absorption capability.

In Figure 4, for reference windshield models with or without the PVB interlayer and at $D/t = 0.62$, the radial crack characteristics are compared. Here, the crack length C is normalized by the characteristic plate length as C/a, and the crack angle is defined in Figure 4[1]. From Figure 4, the radial crack is prone to grow near the longer boarder (with crack angle θ about 22 degrees) in a pure glass windshield (with the thickness $t' = 4.76$mm, the same as the overall thickness of a reference PVB laminated windshield). Whereas, the crack tends to propagate near the shorter boarder (with crack angle about 59 degrees) and also the crack length is shorter in a PVB laminated windshield (at the same D/t).

[1] Note that the crack angle here is the one when the crack is fully developed, i.e. the "steady-state"

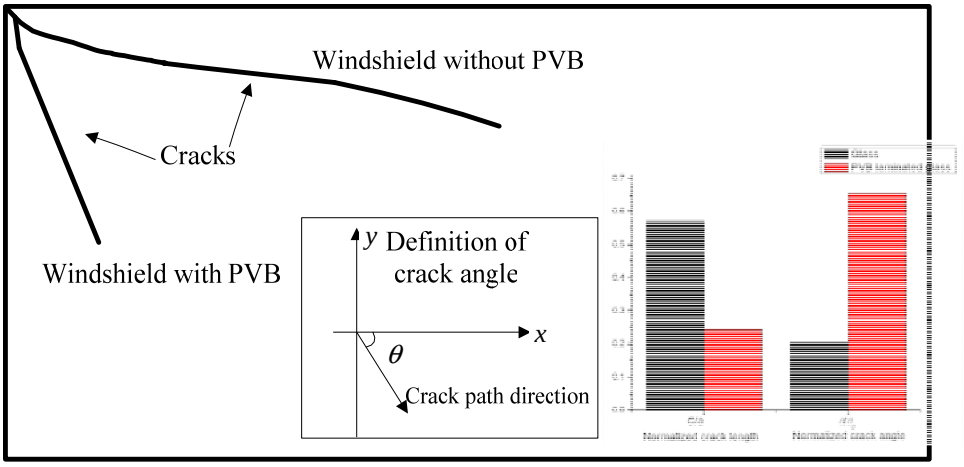

Figure 4: Different crack patterns in reference pure glass windshield and PVB laminated windshield. Values of input parameters of the reference models used in XFEM simulation are listed in Table 1.The normalized steady state crack angle (defined in inset) and length in these two situations are compared at $D/t = 0.62$.

According to Figure 3 and Equation (1), under the same impact speed v, the thicker the PVB interlayer becomes, the smaller D/t is expected owing to the more impact energy mitigated by the thicker PVB interlayer. In other words, to reach the same D/t, a larger v should be imposed on the windshield with thicker PVB interlayer. Consequently, with the help of Equation (1), we convert the relation between C/a and D/t into that between C/a and v/v_0 in Figure 5 (for different PVB interlayer thickness and with other parameters fixed at their reference values). The results demonstrate that under the same v/v_0, the crack length is shorter in a windshield with thicker PVB interlayer. This is consistent with the fact that cracks in the windshield of commercial trucks or buses is shorter (at nearly the same impact speed), which may largely contribute to the thicker PVB interlayer (in cases of similar windshield size with passenger cars) [Xu and Li (2009)]. Unfortunately, the gain (reduction of crack length) becomes less significant as the PVB interlayer becomes very thick, which implies that enhancing energy absorption and reducing crack length may not be achieved simply by thickening the PVB interlayer. Therefore, next we explore the possibility of modifying the PVB material properties.

crack propagation angle.

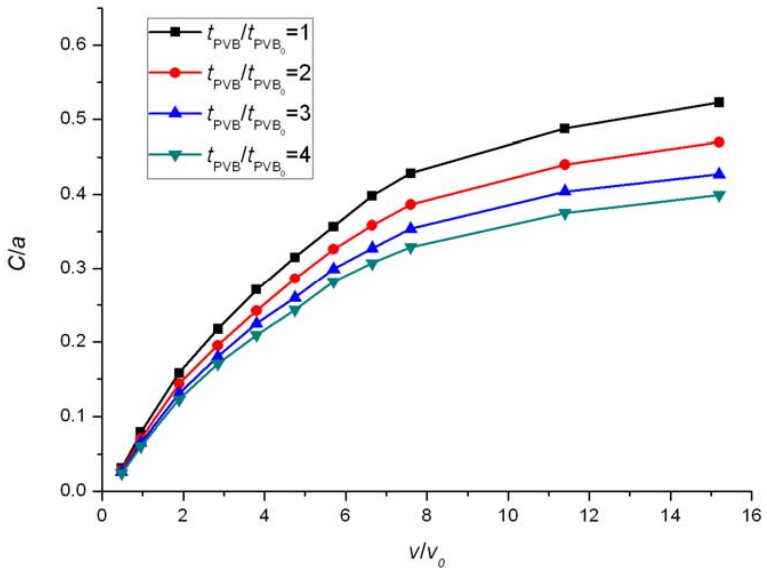

Figure 5: Relations between the normalized crack length and normalized initial impact speed, as the normalized thickness of PVB interlayer varies from 1 to 4. Other parameters used in simulation are the reference values listed in Table 1.

3.1.2 Effect of modified PVB material property

In practice, one may tailor the interlayer material property in terms of better pedestrian protection as well as to further understand its contribution to windshield crack information (which may also help accident reconstruction). As shown in our previous experiment [Xu, Li, Ge, Liu and Zhu (In press); Xu, Li, Liu, Zhu and Ge (In press)], the constitutive behavior of PVB is similar to that of rubber and the uniaxial stress-strain curve can be approximated as $\sigma_{\mathrm{PVB}}\,(\mathrm{MPa}) = 428.9\,(\varepsilon_{\mathrm{PVB}})^{1.832}$, $0 \le \varepsilon_{\mathrm{PVB}} \le 0.525$, where σ_{PVB} and $\varepsilon_{\mathrm{PVB}}$ are stress and strain. In what follows, we generalize the stress-strain relation as $\sigma_{\mathrm{PVB}} = m\kappa\,(\varepsilon_{\mathrm{PVB}})^{n\psi}$ where $\kappa = 428.9\mathrm{MPa}$ and $\psi = 1.832$, and m and n are scale factors – by varying the scale factor m and n, we can perturb the mechanical property of the PVB interlayer (at least in a theoretical way to "strengthen" the PVB layer).

In Figure 6, we vary m and n from 1 to 3 in several different combinations to inspect the influences over C/a. Results show that C/a gets longer when m is smaller or when n is larger (i.e. when the interlayer material is more "compliant"). In other words, in addition to thickening the PVB layer, making the interlayer "stiffer" may also shorten the crack, which implies better pedestrian/passenger protection in

traffic accident.

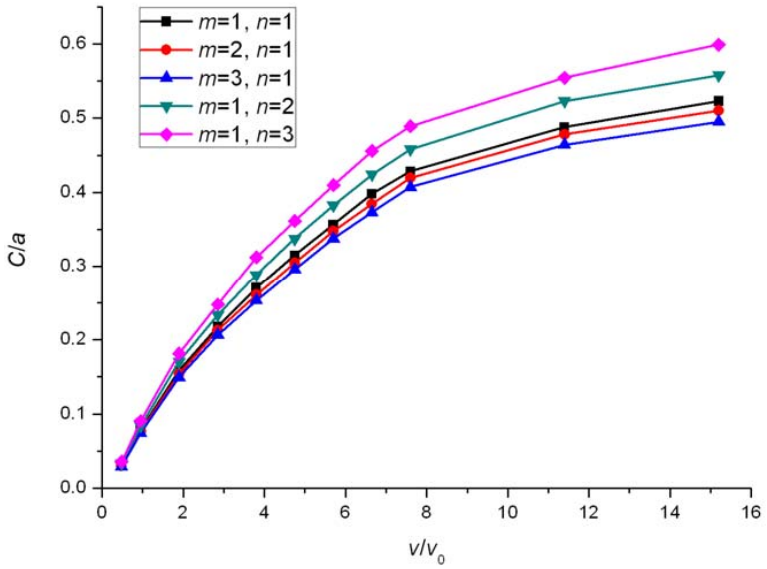

Figure 6: Relations between the normalized crack length and normalized initial impact speed, as the interlayer material scale factors m and n are varied. Other parameters used in simulation are the reference values listed in Table 1.

3.2 Effects of windshield geometrical parameters

In this section, we vary the curvature, the length/width aspect ratio, and the dimension of windshield separately. The results will help to more clearly reveal the relationship between these geometric factors and the crack parameters (e.g. the angle of the longest radial crack).

3.2.1 Effect of curvature of windshield

The main advantage of curvature design of windshield is to keep the whole vehicle in a good aero-dynamics condition. We examine whether the curvature is influential to the crack length in order to further assess its benefit from a mechanical point of view. Here, α is defined as the curvature parameter in Figure 2, which can be normalized by the reference value $\alpha_0 = \pi/2$. In general, under the same impact condition, the crack length tends to be shorter with the increase of α. In essence, with the enhancement of curvature, the magnitude of stress field upon impact is

reduced due to the reduction of head displacement D/t (at the same impact speed), which would favor a shorter crack.

Figure 7 shows the normalized crack length at different curvature parameters (all other parameters are kept at their reference values in Table 1 except for the curvature α). The shorter crack length at larger windshield curvature implies better PVB energy dissipation capability and fracture resistance at the same head displacement. The steady-state crack propagation angle (defined in Figure 4 and normalized by the reference value $\theta_0 = \pi/2$) also changes a lot during the variation of curvature, shown in Figure 8 (with $D/t = 1.21$).

The results indicate that the larger windshield curvature makes the radial crack propagation incline to the longer boarder. From fitting of the XFEM analysis results, the relationship between normalized α and θ can be found as (for the current ranges of parameters)

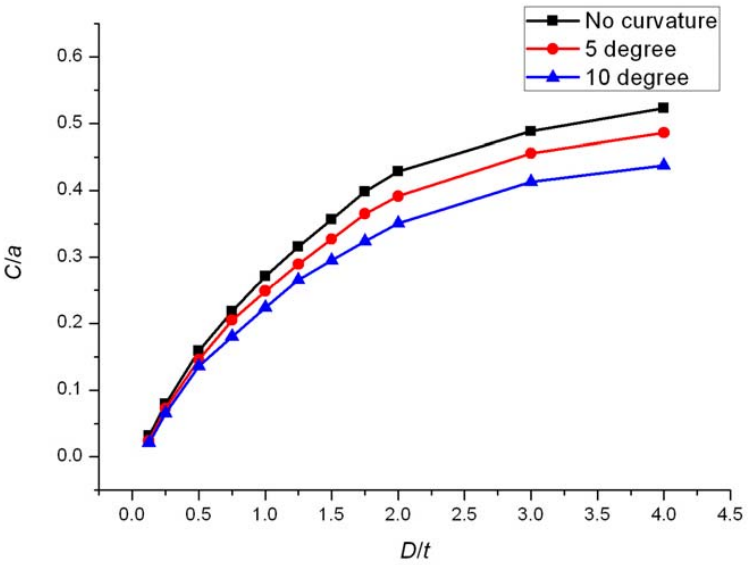

Figure 7: Relations between the normalized crack length and normalized displacement of head into windshield, as the windshield curvature angle is changed 0 to 10 degrees (see Figure 2 for definition of the curvature angle). Other parameters used in simulation are the reference values listed in Table 1.

$$\theta/\theta_0 = e^{-1.398-85.63(\alpha/\alpha_0)^{1.5}-0.777(\alpha/\alpha_0)^{0.5}} \tag{2a}$$

$$\theta/\theta_0 = 2.08\left(4.03+(\alpha/\alpha_0)^{1.06}\right)^{0.5} - 0.530\left(2.89+(\alpha/\alpha_0)^{0.470}\right)^{1.5} - 0.932 \tag{2b}$$

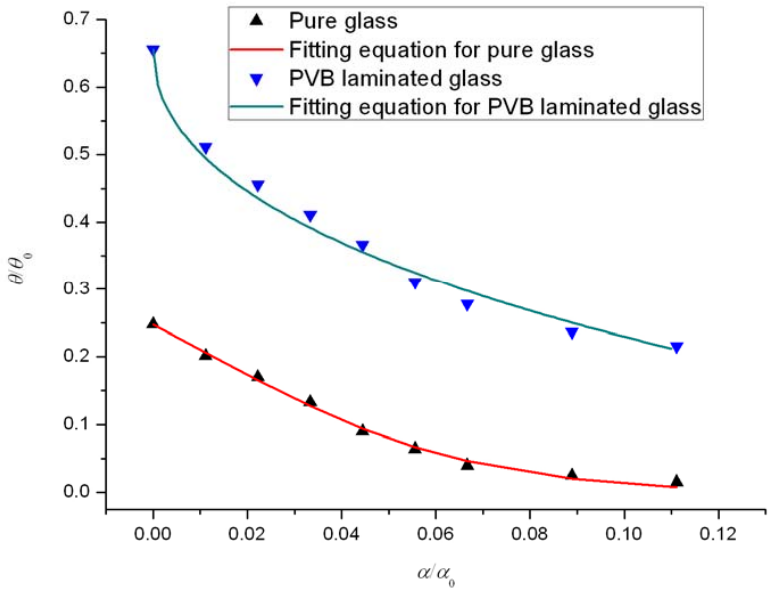

Figure 8: Relations between the normalized crack angle and windshield curvature for both PVB laminated windshield and pure glass windshield. Solid lines denote the fitted results. Other parameters used in simulation are the reference values listed in Table 1.

where Equation (2a) is for pure glass while Equation (2b) is for PVB laminated glass.

3.2.2 *Effect of aspect ratio of length to width of windshield*

The aspect ratio of windshield imposes an effect on crack patterns through the boundary constraint. It is changed through fixing the total area ($a \times b$) while varying a and b simultaneously. Numerical simulations are divided into two sets: pure glass windshield and PVB laminated windshield. All other parameters are fixed at their reference values (see Table 1) and for $D/t = 1.21$. The variation of crack angle as a function of the aspect ratio χ ($\chi = a/b$) is given in Figure 9.

For the scenario of pure glass windshield, the relation between θ and χ can take the following form (for the current ranges of parameters)

$$\theta = 0.9934 \arctan(1/\chi) \tag{3}$$

which indicates that the crack angle θ is almost aligned with the diagonal direction of the windshield, and the crack angle increases as the aspect ratio decreases.

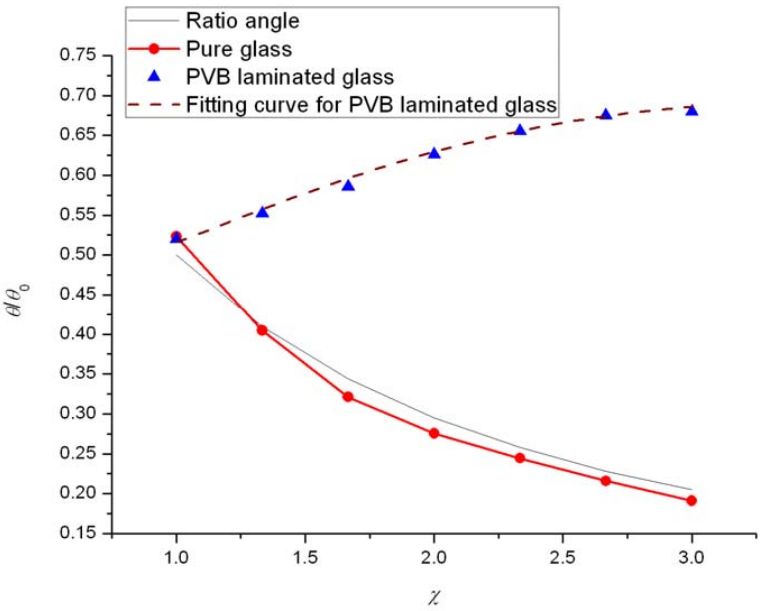

Figure 9: The steady state crack angle as a function of the windshield aspect ratio for PVB laminated windshield and pure glass panel. Other parameters used in simulation are the reference values listed in Table 1. Here the ratio angle denotes a/b.

On the contrary, the crack angle increases as χ increases in a PVB laminated windshield. It is also noticeable from Figure 9 that the variation of the normalized crack angle in a PVB laminated windshield is within a relatively small region (when the aspect ratio of the windshield is changed); in particular, when the aspect ratio is within that of common windshields (where typically χ varies between 2 and 2.5, for which the computed crack angle varies about 7.46%), which may be appreciated for accident reconstruction.

Likewise, the relation between θ/θ_0 and χ for a PVB laminated windshield can take the following form (for the current ranges of parameters)

$$(\theta/\theta_0) = 2.08\left(1.00+(\chi)^{1.31}\right)^{0.5} - 0.530\left(1.00+(\chi)^{0.747}\right)^{1.5} - 0.932 \tag{4}$$

3.2.3 Effect of windshield panel size

Besides the windshield aspect ratio, the dimension of the windshield also varies in different automobiles. In most modern passenger cars (focus of this paper), the

ratio between the dimension of head and windshield (λ) is about 0.03 under the definition of $\lambda = \frac{\text{Projection area of head}}{\text{Projection area of windshield}}$. By fixing the head dimension and aspect ratio of the windshield, we vary $\lambda = 0.005 \sim 0.1$. Figure 10 illustrates the resulting crack length as a function of v/v_0 under different values of λ with the help of Equation (1). Under the same impact speed, the smaller the windshield size is, the longer the normalized crack length is. In essence, because the impact can result in a local stress concentration (which is the driving force for crack propagation), the size of such a prominent impact stress zone is relatively smaller if the windshield is larger, and that will lead to a shorter normalized crack length (although the absolute length of the crack is still longer owing to the larger D/t at the same v/v_0). Note that the effect of λ will gradually decrease as the windshield size is larger. According to the census data in NTADTU, passenger cars have $0.028 \leq \lambda \leq 0.034$ while shuttles and buses have $0.005 \leq \lambda \leq 0.025$. Therefore, within the range of λ for passengers the variation of crack length is relatively small, and during the reconstruction of pedestrian-vehicle accident based on crack analysis, an accident investigator may not need to treat the dimension of windshield as a dominant factor. However, one needs to be cautious to use the crack information to reconstruct accidents with buses and take into account the effect of windshield size.

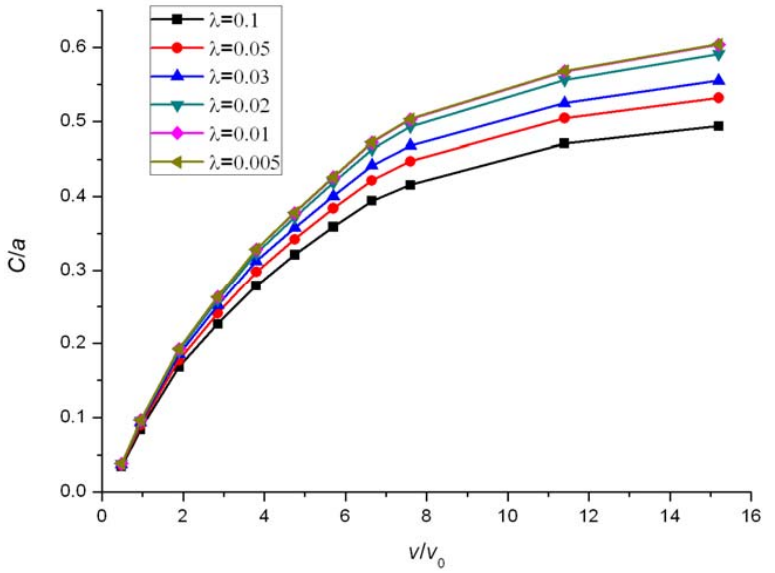

Figure 10: nfluence of the windshield size on the normalized crack length, when the normalized size parameter changes from 0.005 to 0.1 and as the impact velocity is varied. Other parameters used in simulation are the reference values listed in Table 1.

3.3 Effects of boundary conditions

3.3.1 Different supporting ways and materials

In a real world vehicle, the windshield is usually supported and surrounded by a rubber material (Polyurethane) and Ref. [Mkrtchyan and Maier (2007)] provides us a valuable stress-strain data on the three-point bending test of polyurethane, including the failure strength and failure strain. In this section, we let the edge of the reference windshield to be bounded by the polyurethane material (like a saddle-bar that is found in real-world automobiles).

To simplify the problem, we proportionally perturb the original stress of polyurethane σ_0 to a new value σ while assuming the corresponding strain remains a constant. By following the same numerical approach, one can calculate the radial crack pattern for different boundary constraints (while keeping all other governing parameters at their reference values in Table 1). With softer supporting material (i.e. smaller scale factor σ/σ_0) or equivalently looser boundary condition, the maximum displacement of head during impact will be larger under the same initial impact speed. With the help of Eq. (1), we plot the relation between v/v_0 and C/a in Figure 11. It is found that currently widely employed polyurethane material in windshield saddle bar provides a boundary constraint that is "stronger" than simple supported condition but "weaker" than clamped constrain; similar results were found in Ref. [Yuan and Li (2005)]. The normalized crack length can be up to 5% shorter in the simple supported case than in clamped one under the same impact speed. Thus, boundary condition has relatively insignificant influence over crack length. For accident investigators, one may choose to ignore the effect of boundary conditions in different vehicles.

3.3.2 Effect of off-center impact

Off-center impact is very common in real-world accident, yet there was no previous effort to evaluate the cracks in a windshield induced by off-center impact. In this section, we assume that the off-center impact location is still along the x-axis, and denote s as the distance measured from center of windshield to the impact location. A normalized offset distance is defined as $\mu = 2s/a$.

In Figure 12, an example of off-center impact-induced crack XFEM simulation (with the reference parameters listed in Table 1) is demonstrated with $D/t = 1.21$ and μ =0.6. In general, since the crack propagation is mainly affected by the local stress field, one may divide the windshield plate into four subsections (with respect to the off-center impact location), and regard the crack extension in each subsection approximately follows that of a center impact in a windshield with four times the

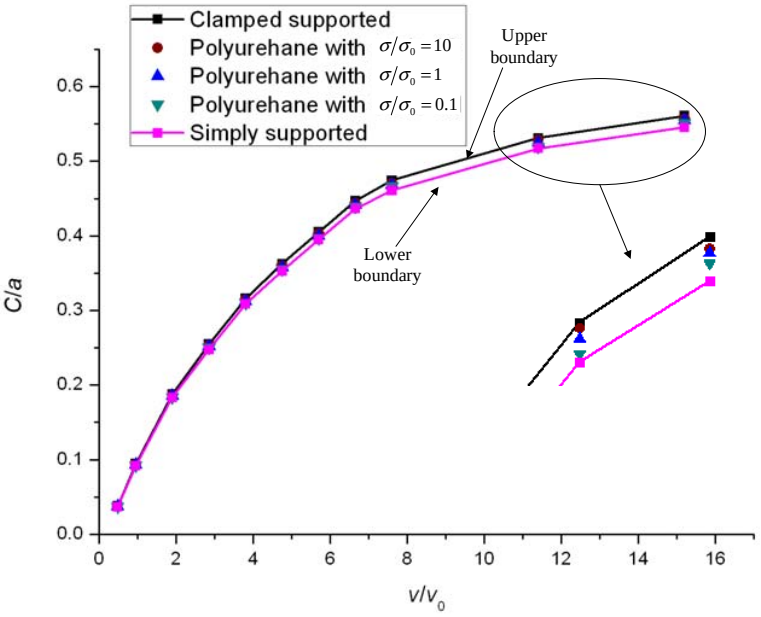

Figure 11: Influence of saddle bar (boundary supporting) material on the normalized crack length, as the impact speed is varied. Other parameters used in simulation are the reference values listed in Table 1. The clamped and simple supported boundary conditions represent the upper and lower bounds for present simulation (in terms of the crack length).

subsection dimension[2]. Indeed for the cracks simulated in Figure 12, each radial crack branch grows roughly according to the unique geometrical characteristics (aspect ratio and size) of the corresponding subsection. Since the crack lengths and angles are different in the four subsections, we let C_s to be the simulated crack length (under the off-center impact) in a given subsection, while let C_f to be the crack length resulted from a center impact of the twofold-sized subsection, and then the averaged C_s/C_f is obtained for all four subsections.

We vary μ in relatively large ranges and Figure 13 indicates that the difference between C_s and C_f will become larger as the impact point is farther away from the center point.

Meanwhile, if the impact point is not too far away from the center of windshield, an accident investigator may divide the windshield into four subsections and analyze

[2] Such an approximation is valid if the normal impact is not too far away from the center and when the windshield curvature is not large.

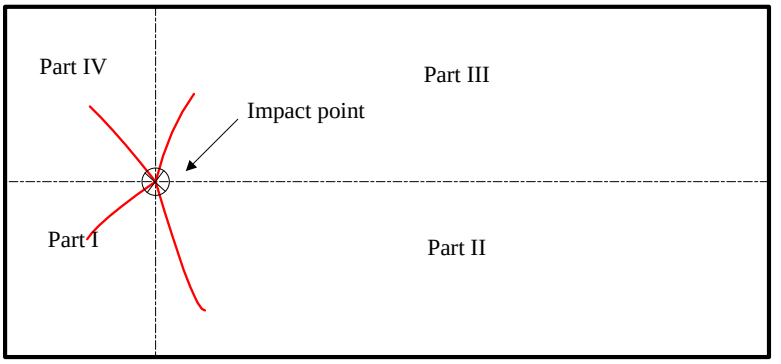

Figure 12: The radial crack pattern simulated using XFEM upon $D/t = 1.21$ and off-center parameter m=0.6. Other parameters used in simulation are the reference values listed in Table 1. When the impact is off-center, crack propagation is no longer symmetric. The crack in each subsection grows in a way that is roughly consistent with that from a fourfold-sized windshield upon center impact.

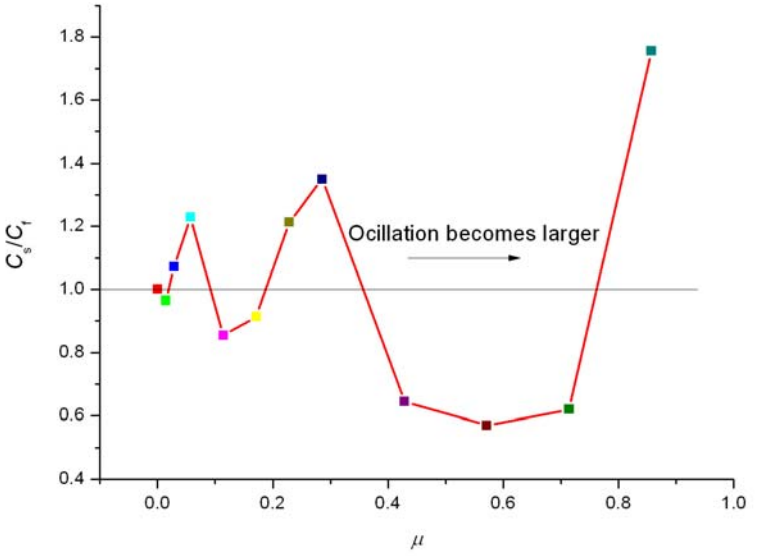

Figure 13: The oscillation in C_s/C_f becomes larger when the impact is more off-center.

the cracking behavior in any subsection; the summarization of the investigation in all four subsections should give reasonable upper and lower bounds of the impact speed.

3.3.3 Inclined impact

In a real-world pedestrian-vehicle accident, the vehicle front-end shape, pedestrian's height and vehicle impact speed will all impose influences over the impact angle of the pedestrian's head. Therefore, the impact angle ϑ is another important variable to the crack pattern on the windshield. We assume the inclined impact occurs at the center of windshield, and first compute the x, y and z deformation response (without cracking) under different impact angles at a fixed total impact speed. Take x-o-z plane for example. The impact angle varies from $\vartheta = 90^\circ$ to $\vartheta = 15^\circ$ ($\vartheta = 0^\circ$ is not included since no displacement will occur in z direction). The impact speed in the y direction maintains 0 while the total impact speed of x, z direction ($\vec{v} = \vec{v}_x + \vec{v}_z$) keeps the same; we investigate two scenarios with $|\vec{v}|$= 10m/s and 20m/s, respectively.

We first check the normalized displacements in x, y and z directions according to different impact angles at different impact speeds (see Figure 14). Obviously, the displacement increases as the velocity becomes larger in the respective direction. Figure 15 shows the normalized crack lengths under a variety of normalized crack angles (ϑ/ϑ_0 where $\vartheta_0 = 90^\circ$). It is found that when the impact angle is larger, the crack length is shorter; that is, the crack length is mainly affected by the resulting head displacement in z direction. Note that in the inclined scenario, cracks grow asymmetrically and we only show the longest crack branch; in other words, for a center impact if the radial crack shows strong asymmetry it may be induced by inclined impact.

3.4 Circumferential crack pattern

In previous sections, the radial crack characteristics under the influences of different geometrical, material, impact conditions, and boundary constraints are discussed. In this section, we investigate the second stage of crack propagation, the circumferential fracture (after the radial cracks are developed). As mentioned in Section 2.2, by the end of the first step of radial crack propagation, the stress field is retrieved to enable the circumferential cracks (which are grown out of closely-spaced small random defects along the previously developed radial crack, without the need of any additional external loads; see Ref. [Xu, Li, Chen, Yan, Ge, Zhu and Liu (2010)] for details).

Figure 16 shows a typical full crack pattern (radial and circumferential) in a PVB laminated windshield (with reference parameters listed in Table 1) subject to human

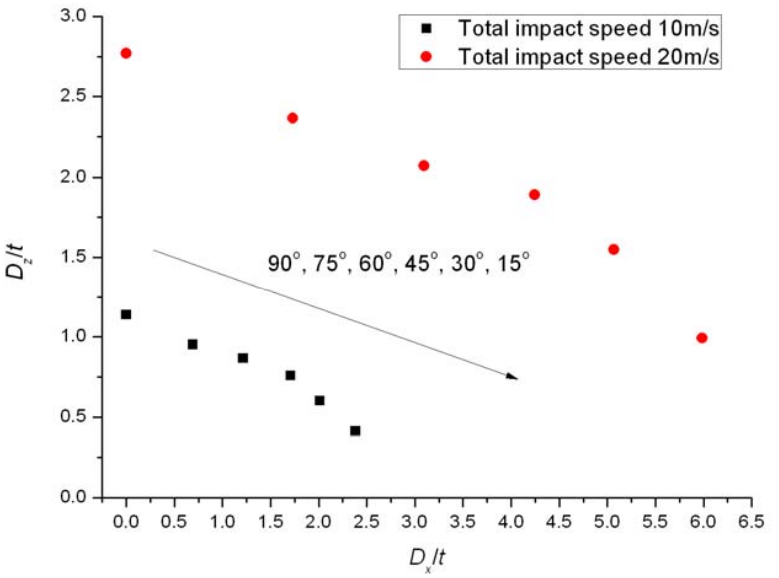

Figure 14: The normalized displacement components in x and z directions under different impact angles, when the total impact speed is either 10m/s or 20m/s. Other parameters used in simulation are the reference values listed in Table 1.

head normal and center impact ($D/t = 1.21$). We can see that the largest circumferential crack initiates from the outmost tip of the radial crack, and there is also a smaller closed circumferential crack near the impact crater. In addition, a few less developed partial circumferential cracks are located in between the two full cracks. It is worthy to point out that the "spider-web crack" is sometimes observed on the real-world windshield [Zhao, Dharani, Liang, Chai and Barbat (2005)], which includes many radial cracks and a few circumferential cracks crossing each other. The reason may be due to multiple contacts which is not considered in this study. The radial crack referred in this study corresponds to the longest one in the real-world windshield cracking, which was shown to have good agreement with real-world accidents [Xu, Li, Chen, Yan, Ge, Zhu and Liu (2010)].

The aspect ratio γ between the major and minor axis of the elliptical circumferential crack (see Figure 16) is an effective indicator for the shape of crack pattern. Figure 17 shows the results of effects of different variables on aspect ratio γ (where in each figure only one parameter in the x-axis is changed and others are fixed at their reference values). Under the conditions of more compliant PVB layer, looser boundary constraint, or larger windshield curvature, the aspect ratio γ becomes closer to 1 (approaching a circle). In essence, the circumferential crack shape is

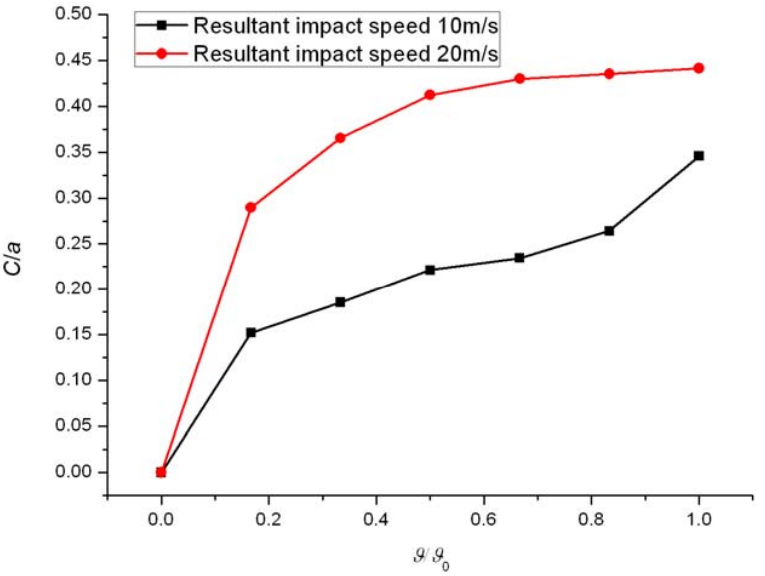

Figure 15: The normalized crack length as a function of the inclined impact angle, for two different total impact speeds. Other parameters used in simulation are the reference values listed in Table 1.

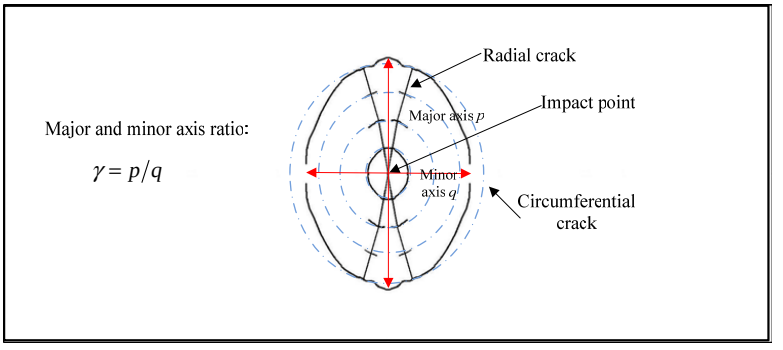

Figure 16: The complete radial and circumferential crack pattern in PVB laminated windshield at $D/t = 1.21$ in XFEM simulation (with reference parameters in Table 1). g is defined as the ratio between the major (y) and minor (x) axes of the elliptical circumferential crack.

to some extent related to the prior radial crack growth, and thus γ depends somewhat on the radial crack angle (θ/θ_0) and length (C/a). Nevertheless, the trends in Figure 17 show that owing to the complicated interaction between hoop and radial stress fields during the two-stage crack propagation, the effects of various material and system parameters are mixed (coupled) and thus the circumferential crack shape is not determined solely by the previous radial crack parameters.

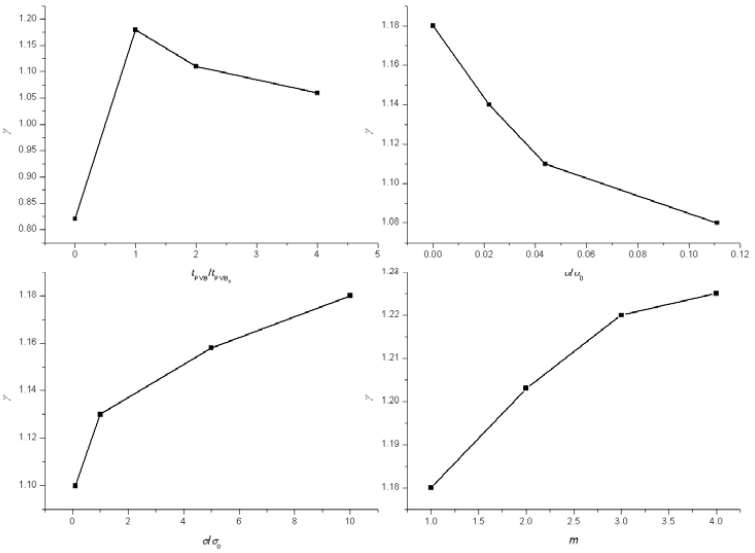

Figure 17: Influences of the normalized PVB interlayer thickness, windshield curvature, supporting material stiffness, and interlayer material stiffness factor on the circumferential crack ratio g. Other parameters used in simulation are the reference values listed in Table 1.

3.5 Governing parameters of crack pattern in windshield

When the results above are combined, the crack pattern characteristics (including the radial crack length and angle, and circumferential crack number and aspect ratio) can be expressed as a function of several main geometrical, material and boundary factors, approximated in a dimensionless functional form as

$$[C/a, \theta/\theta_0, \gamma] = F\,[D/t, \alpha/\alpha_0, \chi, \lambda, \vartheta/\vartheta_0, \mu, \sigma/\sigma_0, (m,n)] \tag{5}$$

where D/t is expressed in terms of M/M_0, v/v_0 and t_{PVB}/t_0 (Eq. (1)).

If we assume that the automobile industry uses the same PVB interlayer material with the same boundary condition (and indeed the boundary's effect is minor, Section 3.3.1), then the above relationship can be simplified as the following for center impact:

$$[C/a, \theta/\theta_0, \gamma] = F'[D/t, \alpha/\alpha_0, \chi, \lambda, \vartheta/\vartheta_0] \tag{6}$$

The variables in the left side of Equation (6) can describe the entire crack pattern effectively while the variables in the right side denote the governing impact, material, and geometric conditions and parameters. Next, we fit the three crack pattern parameters separately[3].

(1) For the crack length $[C/a] = f[D/t, \alpha/\alpha_0, \chi, \lambda, \vartheta/\vartheta_0]$, which is affected by all variables on the right side and can be expressed as (for the ranges of parameters employed in this study):

$$\begin{aligned} C/a = &-0.198\left[(D/t)^{2.56} + (\alpha/\alpha_0)^{0.551} + (\chi)^{-0.0806} + (\lambda)^{7.81} + (\vartheta/\vartheta_0)^{34.7}\right]^{0.5} \\ &+0.141\left[(D/t)^{0.911} + (\alpha/\alpha_0)^{10.26} + (\chi)^{-0.0306} + (\lambda)^{1.23} + (\vartheta/\vartheta_0)^{0.765}\right]^{1.5} \\ &-0.118 \end{aligned} \tag{7}$$

where D/t can be found from Equation (1). Correlation coefficient is $R = 0.9960$.

(2) For the crack angle $[\theta/\theta_0] = g[D/t, \alpha/\alpha_0, \chi, \lambda, \vartheta/\vartheta_0]$, we assume that the steady state crack propagation direction is essentially insensitive to the depth of head displacement into windshield, i.e. $[\theta/\theta_0] = g[\alpha/\alpha_0, \chi, \lambda, \vartheta/\vartheta_0]$. By nonlinear curve fitting, we can obtain:

$$\begin{aligned} \theta/\theta_0 = &2.08\left[(\alpha/\alpha_0)^{1.06} + (\chi)^{1.31} + (\lambda)^{1.76} + (\vartheta/\vartheta_0)^{-0.0262}\right]^{0.5} \\ &-0.530\left[(\alpha/\alpha_0)^{0.470} + (\chi)^{0.747} + (\lambda)^{1.99} + (\vartheta/\vartheta_0)^{-0.00615}\right]^{1.5} - 0.932 \end{aligned} \tag{8}$$

Correlation coefficient is $R = 0.9999$.

[3] In previous sections when we discuss the effect of a variable, we often keep the other variables fixed at their reference values. During the fitting process in this section, all relevant parameters are varied concurrently so that the findings are more general. For example, we vary $D/t, \alpha/\alpha_0, \chi, \lambda, \vartheta/\vartheta_0$ concurrently (in their respective ranges defined in previous sections) and establish a large database of crack geometries based on extensive XFEM simulations, and then we come up with the fitting equations (7)-(9).

(3) The circumferential crack aspect ratio is also assumed to be independent with D/t, and thus $[\gamma] = h[\alpha/\alpha_0, \chi, \lambda, \vartheta/\vartheta_0]$. It can be fitted by

$$\begin{aligned}\gamma = &-0.114\left[(\alpha/\alpha_0)^{0.203} + (\chi)^{-24.8} + (\lambda)^{0.0846} + (\vartheta/\vartheta_0)^{0.476}\right]^{0.5} \\ &-0.716\left[(\alpha/\alpha_0)^{2.48} + (\chi)^{0.00707} + (\lambda)^{-0.00182} + (\vartheta/\vartheta_0)^{-0.0110}\right]^{1.5} + 5.05\end{aligned} \tag{9}$$

Correlation coefficient is $R = 0.9968$.

Equations (7)-(9) indicate the general form and extent of influences from several governing variables. In practice, based on the crack pattern in PVB laminated windshield, the inverse analyses of Equations (7)-(9) may lead to the determination of relevant information including impact speed, windshield material and geometrical properties, etc., which may be helpful for both accident investigators and vehicle crashworthiness designers.

4 Concluding Remarks

Crack pattern formed in windshield upon head impact has been a hot yet unsolved problem for a long time, since it is very critical for accident reconstruction, vehicle crashworthiness analysis, and pedestrian and passenger protection. Using XFEM simulations, we carry out an extensive study on PVB laminated windshield crack pattern (including both radial and circumferential cracks). The effects of the most prominent material, geometric, and impact conditions and parameters are explored.

Based on systematic numerical simulations, explicit relations are established between the crack characteristics and prominent material/system parameters. To summarize, among the various parameters considered in this study, we propose a map that bridges the most influential parameters and the crack pattern in Figure 18. The map is established based on the extensive XFEM simulations in this study. Furthermore, as each governing factor is varied, the qualitative impact on the crack geometry is summarized in Table 2. Together, Figure 18 and Table 2 can provide an overall qualitative view of the numerical results in this paper (the quantitative results are related to Equations (7)-(9)).

The results may provide accident investigators and vehicle safety designers some fundamental insights on the general relations between governing material/system variable and crack patterns, in particular the effects of single variable and combination of several variables.

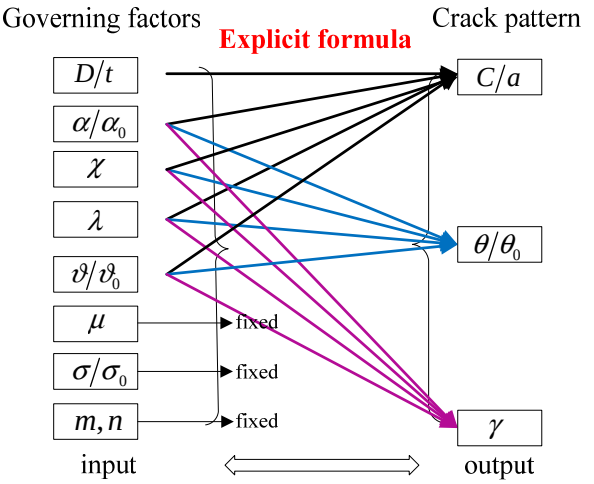

Figure 18: Bridging the main material and system parameters with PVB laminated windshield crack pattern.

Table 2: Summary of qualitative relationship between governing variables and crack pattern parameters

		Governing material/system variables								
		D/t	α/α_0	χ	λ	ϑ/ϑ_0	μ	σ/σ_0	m	n
Crack pattern parameter	C/a	↗↗	↗↙	↗↙	↗↙	↗↗	-	↗↗	↗↙	↗↗
	θ/θ_0	-	↗↙	↗↗	↗↗	↗↙	-	-	-	-
	γ	-	↗↙	↗↗	↗↙	↗↗	-	↗↗	↗↗	↗↙

Note:

"↗↗" stands for the scenario that the increase of one variable will cause the increase of the other one (and vice versa).

"↗↙" stands for the scenario that the increase of one variable will cause the decrease of the other one (and vice versa).

"-" stands for the scenario that the relationship between two variables are oscillating (such as cases involving μ) or very weak (one variable will almost keep a constant when the other variable changes).

Acknowledgement: This work is financially supported by National Natural Science Foundation of China (NSFC 10972122), State Key Laboratory of Automotive Safety & Energy, Tsinghua University (ZZ0800062) and Doctoral Fund of Ministry of Education of China (20090002110082). Y. Li and X. Chen appreciate the founding from Tsinghua University under the International Cooperation Project. J. Xu also appreciates China Scholarship Council (CSC) to financially sponsor his study at Columbia University through a joint Ph.D. program. X. Chen is supported by the National Science Foundation (CMMI-0643726) and NSFC (50928601).

References

Akrout A.; Hammami L.; Tahar M. B.; Haddar M. (2008): Inter-facial shear effects of ultra-thin film on laminated glass plate dynamical behaviour. *Proceedings of the Institution of Mechanical Engineers Part C-Journal of Mechanical Engineering Science*, vol. 222, no. 8, pp. 1421-1433.

Asik M. Z.; Tezcan S. (2005): A mathematical model for the behavior of laminated glass beams. *Comput. Struct.*, vol. 83, no. 21-22, pp. 1742-1753.

Asik M. Z.; Tezcan S. (2006): Laminated glass beams: Strength factor and temperature effect. *Comput. Struct.*, vol. 84, no. 5-6, pp. 364-373.

Belytschko T.; Black T. (1999): Elastic crack growth in finite elements with minimal remeshing. *Int. J. Numer. Methods Eng.*, vol. 45, no. 5, pp. 601-620.

Du Bois P. A.; Kolling S.; Fassnacht W. (2003): Modelling of safety glass for crash simulation. *Comput. Mater. Sci.*, vol. 28, no. 3-4, pp. 675-683.

Herndon G.; Allen K.; Roberts A.; Phillips D.; Batzer S. A. (2007): Automotive side glazing failure due to simulated human interaction. *Eng. Fail. Anal.*, vol. 14, no. 8, pp. 1701-1710.

Holand W.; Beall G. H. (2002): *Glass Ceramic Technology*. Wiley-Blackwell, 2002.

Ivanov I. V. (2006): Analysis, modelling, and optimization of laminated glasses as plane beam. *Int. J. Solids Struct.*, vol. 43, pp. 6887-6907.

Jacob G. C.; Starbuck J. M.; Fellers J. F.; Simunovic S.; Boeman R. G. (2006): Crashworthiness of various random chopped carbon fiber reinforced epoxy composite materials and their strain rate dependence. *J. Appl. Polym. Sci.*, vol. 101, no. 3, pp. 1477-1486.

Mkrtchyan L.; Maier M. (2007): Fibre reinforced polyurethane foam to increase passive safety of vehicle occupants. *Plastics Rubber and Composites*, vol. 36, no. 10, pp. 445-454.

Moes N.; Dolbow J.; Belytschko T. (1999): A finite element method for crack

growth without remeshing. *Int. J. Numer. Methods Eng.*, vol. 46, no. 1, pp. 131-150.

Muralidhar S.; Jagota A.; Bennison S. J.; Saigal S. (2000): Mechanical behaviour in tension of cracked glass bridged by an elastomeric ligament. *Acta Mater.*, vol. 48, no. 18-19, pp. 4577-4588.

Ogasawara N.; Chiba N.; Chen X. (2006): Limit Analysis-Based Approach to Determine the Material Plastic Properties with Conical Indentation. *Journal of Materials Research*, vol. 21, pp. 947-958.

RahulKumar P.; Jagota A.; Bennison S. J.; Saigal S. (2000): Interfacial failures in a compressive shear strength test of glass/polymer laminates. *Int. J. Solids Struct.*, vol. 37, no. 48-50, pp. 7281-7305.

Seshadri M.; Bennison S. J.; Jagota A.; Saigal S. (2002): Mechanical response of cracked laminated plates. *Acta Mater.*, vol. 50, no. 18, pp. 4477-4490.

Sun X.; Khaleel M. A. (2005): Effects of different design parameters on the stone-impact resistance of automotive windshields. *Proceedings of the Institution of Mechanical Engineers Part D-Journal of Automobile Engineering*, vol. 219, no. D9, pp. 1059-1067.

Sun X.; Liu W. N.; Chen W. N.; Templeton D. (2009): Modeling and characterization of dynamic failure of borosilicate glass under compression/shear loading. *Int. J. Impact Eng*, vol. 36, no. 2, pp. 226-234.

Timmel M.; Kolling S.; Osterrieder P.; Bois P. A. D. (2007): A finite element model for impact simulation with laminated glass. *Int. J. Impact Eng*, vol. 34, no. 8, pp. 1465-1478.

Valera T. S.; Demarquette N. R. (2008): Polymer toughening using residue of recycled windshields: PVB film as impact modifier. *Eur. Polym. J.*, vol. 44, pp. 755-768.

Van Slycken J.; Verleysen P.; Degrieck J.; Bouquerel J.; De Cooman B. C. (2006): Crashworthiness characterization and modeling of high-strength steels for automotive applications. *Proceedings of the Institution of Mechanical Engineers Part D-Journal of Automobile Engineering*, vol. 220, no. D4, pp. 391-400.

Wei J.; Dharani L. R. (2006): Response of laminated architectural glazing subjected to blast loading. *Int. J. Impact Eng*, vol. 32, no. 12, pp. 2032-2047.

Wood D. P. (1998): Impact and movement of pedestrian in frontal collisions with vehicles. *Proceedings of institute of Mechanical Engineers, Part D, Automotive Engineering*, vol. 202, pp. 101-110.

Xu H.; Du X.; Xu Y.; Wang L.; Lin Q. (2008): Vehicles' crashing accident reconstruction model based on lamp debris. *Journal of Chang'an University (Natural*

Science Edition), vol. 28, no. 2, pp. 80-83.

Xu J.; Li Y. (2009): Crack analysis in PVB laminated windshield impacted by pedestrian head in traffic accident. *Int. J. Crashworthiness*, vol. 14, no. 1, pp. 63-71.

Xu J.; Li Y. (2009): Study of damage in windshield glazing subject to impact by a pedestrian's head. *Proc. Inst. Mech. Eng. Part D J. Automob. Eng.*, vol. 223, no. 1, pp. 77-84.

Xu J.; Li Y. (2009): Review on pedestrian-vehicle impact accident reconstruction technology. *Automotive Engineering*, vol. 31, no. 11, pp. 1029-1033.

Xu J.; Li Y.; Lu G.; Zhou W. (2009): Reconstruction model of vehicle impact speed in pedestrian-vehicle accident. *Int. J. Impact Eng*, vol. 36, no. 6, pp. 783-788.

Xu J.; Li Y.; Ge D.; Liu B.; Zhu M. (In press): Experimental investigation on constitutive behavior of PVB under impact loading. *Int. J. Impact Eng*,

Xu J.; Li Y.; Liu B.; Zhu M.; Ge D. (In press): Experimental study on mechanical behavior of PVB laminated glass under quasi-static and dynamic loadings. *Composite B*,

Xu J.; Li Y.; Chen X.; Yan Y.; Ge D.; Zhu M.; Liu B. (2010): Characteristics of windshield cracking upon low-speed impact: Numerical simulation based on the extended finite element method. *Comput. Mater. Sci.*, vol. 48, no. 3, pp. 582-588.

Yao J. F.; Yang J. K.; Otte D. (2008): Investigation of head injuries by reconstructions of real-world vehicle-versus-adult-pedestrian accidents. *Saf. Sci.*, vol. 46, no. 7, pp. 1103-1114.

Yuan X.; Li S. M. (2005): Analysis of rectangular thin plate vibration under different support conditions. *Aeroengine*, vol. 31, no. 3, pp. 39-43.

Zhao S.; Dharani L. R.; Chai L.; Barbat S. D. (2006): Dynamic response of laminated automotive glazing impacted by spherical featureless headform. *Int. J. Crashworthiness*, vol. 11, no. 2, pp. 105-113.

Zhao S.; Dharani L. R.; Chai L.; Barbat S. D. (2006): Analysis of damage in laminated automotive glazing subjected to simulated head impact. *Eng. Fail. Anal.*, vol. 13, no. 4, pp. 582-597.

Zhao S.; Dharani L. R.; Liang X.; Chai L.; Barbat S. D. (2005): Crack initiation in laminated automotive glazing subjected to simulated head impact. *Int. J. Crashworthiness*, vol. 10, no. 3, pp. 229-236.